Kinetic and Thermodynamic Acidity of [Cp(NO)(PPh₃)Re(2,5-dimethyl-3-thienyl)carbene]⁺. Transition State Imbalance and Intrinsic Barriers[†]

Claude F. Bernasconi,*,[‡] Santanu Bhattacharya,[‡,§] Philip J. Wenzel,[‡] and
Marilyn M. Olmstead[#]

*Department of Chemistry and Biochemistry, University of California, Santa Cruz, California 95064, and
Department of Chemistry, University of California, Davis, California 95616*

Received May 18, 2006

The synthesis and characterization of [Cp(NO)(PPh₃)Re(2,5-dimethyl-3-thienyl)carbene]⁺ (**3H⁺(S)**), a novel Fischer carbene complex, is described. **3H⁺(S)** undergoes reversible deprotonation with a pK_a of 2.64 in 50% MeCN−50% water (v/v). Rate constants for the deprotonation of **3H⁺(S)** by carboxylate ions and by primary aliphatic and secondary alicyclic amines were determined. A major focus of this paper is a comparison of the kinetic and thermodynamic acidities of **3H⁺(S)** with those of [Cp(NO)-(PPh₃)Re(2-thienyl)carbene]⁺, **1H⁺(S)**. The pK_a of **1H⁺(S)** (2.51) is virtually the same as that of **3H⁺(S)**. This appears to be the result of a fortuitous cancellation of acidity-reducing and acidity-enhancing factors, a conclusion supported by a computational study of gas phase acidities. An analysis of Brønsted plots indicates that the *intrinsic* rate constants for proton transfer are about 2 orders of magnitude lower for **3H⁺(S)** than for **1H⁺(S)**. This reduction is the result of steric effects and of electronic effects connected with the imbalanced nature of the transition state.

Introduction

We have recently reported on the kinetic and thermodynamic acidities of the cationic rhenium carbene complexes **1H⁺(X)** and **2H⁺(X)**.[1,2] A major point of interest was the fact that **1(X)**
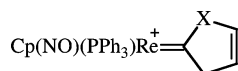
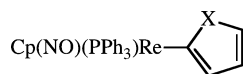**1H⁺(O)** (X = O)　　　　**2H⁺(O)** (X = O)
1H⁺(S) (X = S)　　　　**2H⁺(S)** (X = S)
1H⁺(Se) (X = Se)
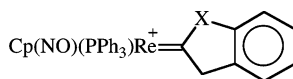
and **2(X)**, the respective conjugate bases of these carbene

1(O) (X = O)　　　　**2(O)** (X = O)
1(S) (X = S)　　　　**2(S)** (X = S)
1(Se) (X = Se)
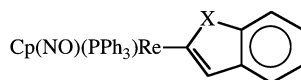
complexes, represent derivatives of the aromatic heterocycles furan, thiophene, selenophene, benzofuran, and benzothiophene,

respectively, and the question of how their aromaticity affects the intrinsic barriers of the proton transfer.

In this paper we report a kinetic and thermodynamic study of the deprotonation of **3H⁺(S)** by various bases along with

3H⁺(S)　　　　　　　　**3(S)**　　　　　　　　(1)
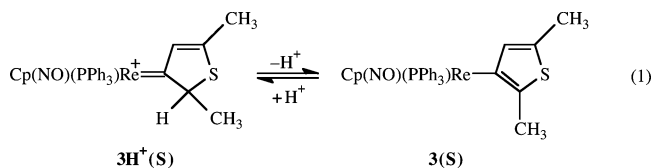
some computational results relating to its thermodynamic acidity. **3H⁺(S)**, which, without methyl groups, represents a constitutional isomer of **1H⁺(S)**, is a new carbene complex. It can be prepared by protonation of **3(S)**, which is a known compound that has been described by Angelici et al.[3]

Results

Synthesis. **3H⁺(S)** was prepared in high yield by protonation of **3(S)** with HBF₄·OMe₂ in cold acetonitrile, as described in more detail in the Experimental Section. The synthesis of **3(S)** led to high-quality crystals, which allowed a determination of its X-ray structure shown in Figure 1; the crystal data are given in the Supporting Information (Tables S1−S5).[4]

Reversibility of Proton Transfer. Both **3H⁺(S)** and **3(S)** are stable for several minutes in pure acetonitrile,[5] which allowed us to determine their UV−vis spectra and demonstrate the reversibility of the proton transfer. Figure 2 displays the UV/vis

---

[†] This is Part 33 of the series Physical Organic Chemistry of Transition Metal Complexes. Part 32: Bernasconi, C. F.; Ragains, M. L. *J. Organomet. Chem.* **2005**, *690*, 5616.

* To whom correspondence should be addressed. E-mail: bernasconi@chemistry.ucsc.edu.

[‡] Santa Cruz.

[§] Present address: Department of Chemistry, Maharaja Manindra Chandra College, Kolkata-700 003, India.

[#] Davis.

(1) Bernasconi, C. F.; Ragains, M. L. *J. Am. Chem. Soc.* **2001**, *123*, 11890.

(2) Bernasconi, C. F.; Ragains, M. L.; Bhattacharya, S. *J. Am. Chem. Soc.* **2003**, *125*, 12328.

(3) (a) Robertson, M. J.; White, C. J.; Angelici, R. J. *J. Am. Chem. Soc.* **1994**, *116*, 5190. (b) White, C. J.; Angelici, R. J. *Organometallics* **1994**, *13*, 5132.

(4) See paragraph concerning Supporting Information at the end of this paper.

(5) The first-order rate constant for decomposition of **3H⁺(S)** in acetonitrile at 25 °C is 5 × 10⁻⁴ s⁻¹.
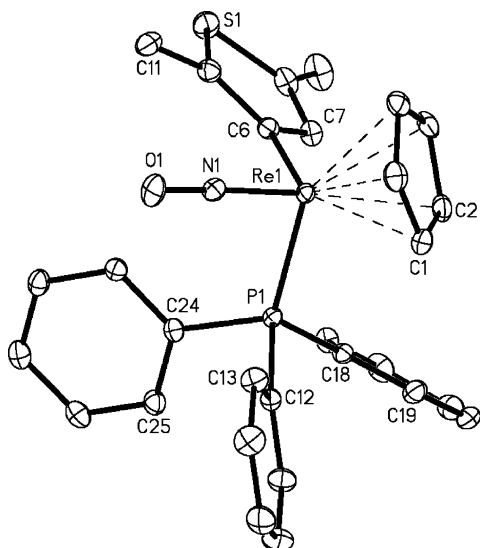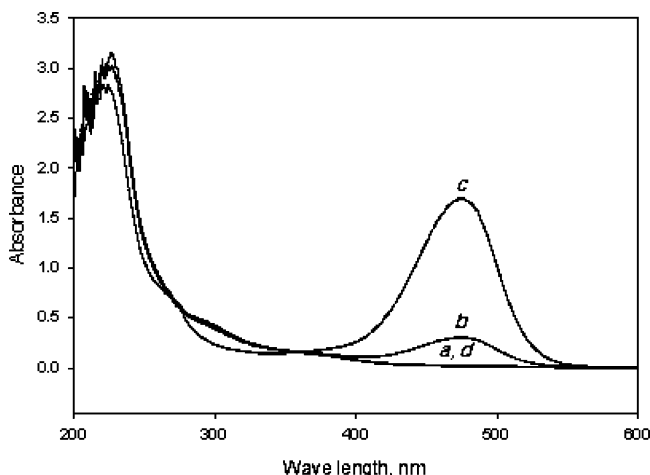
Figure 1. Crystal structure of **3(S)**.

Figure 2. UV/vis spectra in acetonitrile. Spectrum *a* corresponds to **3(S)**; spectrum *b* is obtained after addition of a small amount of trifluoroacetic acid, showing partial conversion of **3(S)** into **3H⁺(S)**; spectrum *c* shows complete conversion to **3H⁺(S)** after addition of excess trifluoroacetic acid; spectrum *d*, which is identical to spectrum *a*, is obtained by adding an excess of piperidine to **3H⁺(S)**.

spectra of both compounds in acetonitrile. The first spectrum (*a*), which shows no absorption at 475 nm, is that of **3(S)**. The second spectrum (*b*) was generated by addition of a small amount of trifluoroacetic acid and represents a mixture of **3(S)** and **3H⁺(S)**. The third spectrum (*c*), with a strong absorption at 475 nm, corresponds to complete conversion of **3(S)** into **3H⁺(S)** after addition of excess acid. When excess piperidine was added to the **3H⁺(S)** solution, spectrum *d* reverted to that of **3(S)**, indicating complete recovery.

The reversibility of the proton transfer was also demonstrated by starting with **3H⁺(S)**, adding excess piperidine for complete conversion to **3(S)**, and complete recovery of **3H⁺(S)** after adding trifluoroacetic acid.

Kinetics of Proton Transfer. A. General Features. Kinetic measurements were carried out in 50% MeCN−50% water (v/v) at 25 °C and an ionic strength of 0.1 M maintained with KCl, the same medium used for the study of **1H⁺(X)** and **2H⁺(X)**.[1,2] Kinetic data were collected in HCl and KOH solutions as well as in carboxylate and amine buffers; all experiments were run under pseudo-first-order conditions with

3H⁺(S) or **3(S)** as the minor component. The observed pseudo-first-order constant for equilibrium approach is given by eq 2,

$$k_{obsd} = k_1^{H_2O} + k_1^{OH}[OH^-] + k_1^B[B] +$$
$$k_{-1}^H a_{H^+} + k_{-1}^{H_2O} + k_{-1}^{BH}[BH] \quad (2)$$

with the various terms defined in eq 3, where B and BH stand for the buffer base and buffer acid, respectively.

$$3H^+(S) \underset{k_{-1}^H a_{H^+} + k_{-1}^{H_2O} + k_{-1}^{BH}[BH]}{\overset{k_1^{H_2O} + k_1^{OH}[OH^-] + k_1^B[B]}{\rightleftharpoons}} 3(S) \quad (3)$$

All reactions except for the ones with aminoacetonitrile as the base were run in a stopped-flow spectrophotometer; the latter were run in a conventional spectrophotometer. As discussed below, the pK_a of **3H⁺(S)** was determined to be 2.64. Hence, most kinetic runs were initiated by mixing a solution of **3H⁺(S)** in pure acetonitrile with an aqueous solution containing the appropriate buffer or KOH solution. Only for the experiments in HCl were the runs initiated by mixing a solution of **3(S)** in pure acetonitrile with the appropriate aqueous HCl solution.

B. Kinetics in HCl and in Neutral Unbuffered Solutions. Rate constants were determined as a function of [HCl] in a pH range from 1.1 to 3.1. In this pH range the only significant terms in eq 2 are those shown in eq 4. The raw data are reported in Table S6.[4]

$$k_{obsd} = k_1^{H_2O} + k_{-1}^H a_{H^+} \quad (4)$$

A plot of k_{obsd} versus a_{H^+} yielded $k_{-1}^H = 3.39 \pm 0.10$ M⁻¹ s⁻¹ and $k_1^{H_2O} \approx 0.019 \pm 0.04$ s⁻¹. A somewhat lower value for $k_{-1}^{H_2O}$, $(7.77 \pm 0.10) \times 10^{-3}$ s⁻¹, was obtained from runs in an approximately neutral unbuffered solution where $k_{obsd} = k_{-1}^{H_2O}$. This latter value is deemed more reliable and is the one adopted in further discussion. From $K_a^{CH} = k_1^{H_2O}/k_{-1}^H = 2.27 \times 10^{-3}$ a pK_a^{CH} of 2.64 ± 0.02 can be calculated.

C. Kinetics in KOH Solution. In KOH solutions the equilibrium strongly favors **3(S)** over **3H⁺(S)**, and hence eq 2 simplifies to eq 5.

$$k_{obsd} = k_1^{OH}[OH^-] + k_1^{H_2O} \quad (5)$$

Rate constants were determined at [KOH] ranging from 0.001 to 0.1 M. The raw data are summarized in Table S7.[4] A plot of k_{obsd} versus [OH⁻] yielded $k_1^{OH} = 53.4 \pm 1.1$ M⁻¹ s⁻¹; the intercept was too small to yield a value for $k_1^{H_2O}$. A value of $k_{-1}^{H_2O} = 4.86 \times 10^{-9}$ s⁻¹ was calculated from $k_{-1}^{H_2O} = k_1^{OH}K_w/K_a^{CH}$, where K_w is the ionic product of the solvent.[6]

D. Kinetics in Amine Buffers. Reactions with the following amines were investigated: *n*-butylamine, 2-methoxyethylamine, glycinamide, 2-chloroethylamine, aminoacetonitrile, piperidine, piperazine, 1-(2-hydroxyethyl)piperazine (HEPA), and piperazine carboxaldehyde (PPAL). The experiments were performed at constant pH with buffer ratios of approximately 1:1. For each amine rates were determined at eight amine concentrations ranging from approximately 0.005 to 0.05 M (Tables S8−S17).[4] All plots of k_{obsd} versus free amine concentration were strictly linear according to eq 6;

(6) $pK_w = 15.19$ in 50% MeCN−50% water (v/v) at 25 °C ($\mu = 0.1$ M KCl).[7]

$$k_{obsd} = k_1^{H_2O} + k_1^{OH}[OH^-] + k_1^B[B] \qquad (6)$$

in most cases the intercept ($k_1^{H_2O} + k_1^{OH}[OH^-]$) was negligible except for the reactions with the least basic amines, where $k_1^{H_2O}$ significantly contributes to k_{obsd} at low amine concentrations. The k_1^B values obtained from the slopes also provided k_{-1}^{BH} values as $k_{-1}^{BH} = k_1^B K_a^{BH}/K_a^{CH}$.

E. Kinetics in Carboxylate Buffers. The following carboxylate buffers were investigated: acetate, methoxyacetate, and chloroacetate. Due to "buffer failure", it was more difficult to maintain a constant buffer ratio in these experiments, especially with the most acidic buffer; that is, for a given series of buffer concentrations, the pH varied somewhat. Because in this pH range the $k_{-1}^H a_{H^+}$ term contributes significantly to k_{obsd}, this necessitated a slight change in the data treatment as follows. Equation 2 in this case simplifies to eq 7, which, after rearrangement, becomes eq 8, where $k_1^{H_2O}$ and $k_{-1}^H a_{H^+}$ are

$$k_{obsd} = k_1^{H_2O} + k_{-1}^H a_{H^+} + k_1^B[B] + k_{-1}^{BH}[BH] \qquad (7)$$

$$k_{obsd}^{corr} = k_{obsd} - k_1^{H_2O} - k_{-1}^H a_{H^+} = k_1^B\left(1 + \frac{a_{H^+}}{K_a^{CH}}\right)[B] \qquad (8)$$

known on the basis of the experiments in HCl and KOH solutions. The raw data are reported in Tables S18–S20.[4] Plots of k_{obsd}^{corr} versus carboxylate ion concentration yielded slopes given by eq 9, from which k_1^B could be calculated.

$$\text{slope} = k_1^B\left(1 + \frac{a_{H^+}}{K_a^{CH}}\right) \qquad (9)$$

Similar experiments were attempted using cyanoacetate, dichloroacetate, and trichloroacetate buffers. However, due to the strong contribution of $k_{-1}^H a_{H^+}$ to k_{obsd}, the experimental uncertainties in the k_1^B and k_{-1}^{BH} values became too large for a precise determination of these rate constants.

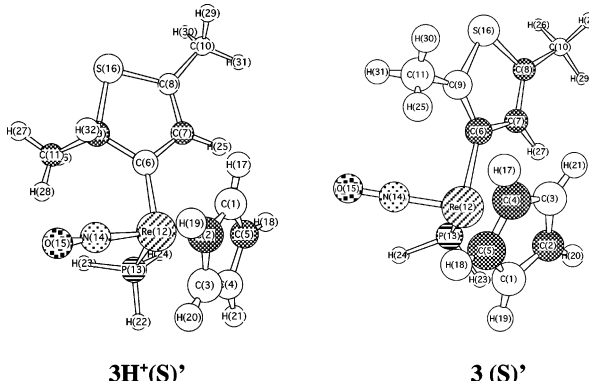**Theoretical Calculations.** Additional insight, in particular with respect to the relative acidities of $3H^+(S)$ and $1H^+(S)$, was sought by performing theoretical calculations. To reduce demand on computer time and still be able to use a reasonably high B3LYP computational level (see Experimental Section), the triphenylphosphine ligand was replaced with PH$_3$, which is not expected to change the electronic effect of this ligand very much. The structures modified in this manner will be identified with a prime, i.e., $1H^+(S)'$, $1(S)'$, etc. Table 1 reports the calculated geometric parameters of $3H^+(S)'$ and $3(S)'$, as well as those of $3(S)$ determined by X-ray crystallography.

The calculated gas phase acidities of $1H^+(S)'$, $3H^+(S)'$, and several analogues with one or two methyl groups are reported in Chart 1. L$_3$ refers to Cp(NO)(PH$_3$). The results of the requisite energy calculations are summarized in Table S21.[4] Note that the larger $\Delta H°$ values indicate lower acidities. Relevant bond lengths for the various structures are reported in Chart 2, while NPA[14] group charges are shown in Chart 3; additional geometric parameters along with the Gaussian output are summarized in Tables S22–S37, while atomic charges are reported in Tables S38–S45.

Table 1. Theoretical and X-ray Geometric Parameters for $3H^+(S)'$, $3(S)'$, and $3(S)$ (X-ray)[a]

3H$^+$(S)'   **3 (S)'**

	$3H^+(S)'$	$3(S)'$	$3(S)$ (X-ray)
Re−C6	2.028	2.144	2.138
Re−N14	1.776	1.767	1.760
Re−P13	2.397	2.344	2.345
Re−C1	2.341	2.271	2.265
Re−C2	2.344	2.341	2.253
Re−C3	2.397	2.315	2.317
Re−C4	2.385	2.399	2.319
Re−C5	2.353	2.427	2.360
N14−O15	1.179	1.192	1.210
C6−C9	1.523	1.379	1.372
S16−C9	1.864	1.766	1.748
C8−S16	1.723	1.744	1.727
C6−C7	1.415	1.449	1.447
C7−C8	1.388	1.370	1.363
∠C6,Re12,P13	90.48	88.06	92.23
∠C6,Re12,N14	95.95	94.88	98.20
∠C6,C9,S16	107.71	111.80	112.01
∠C8,S16,C9	91.39	92.29	92.54
∠C6,C7,C8	116.78	116.16	115.89
∠C7,C8,S16	113.96	109.48	109.60
∠C7,C6,C9	109.94	110.26	109.94

[a] Bond lengths in angstroms and bond angles in degrees.

moiety are crucial in directing the reaction toward $3(S)$; without the methyl groups the reaction leads to $1(S)$ and $1H^+(S)$ according to Scheme 2.[3]

For purposes of reactivity comparison with $1H^+(S)$, it would have been desirable to prepare the corresponding carbene complex without the methyl groups, i.e., $6H^+(S)$. However,

6H$^+$(S)   **6(S)**
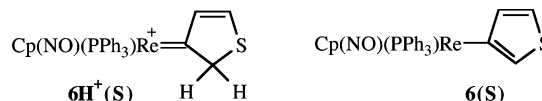
because reaction of **12** with base yields $1(S)$[2,3] instead of $6(S)$, $6H^+(S)$ could not be obtained. The two methyl groups notwithstanding, some interesting comparisons can be made between

(7) Bernasconi, C. F.; Sun, W. *J. Am. Chem. Soc.* **1993**, *115*, 12532.

(8) An erroneous λ_{max} (355 nm) was reported in ref 2.

(9) Fischer, H.; Podschadly, O.; Roth, G.; Herminghaus, S.; Klewitz, S.; Heck, J.; Houbrechts, S.; Meyer, T. *J. Organomet. Chem.* **1997**, *541*, 321.

(10) Bernasconi, C. F.; Ragains, M. L. Unpublished observations.

(11) (a) McMurry, J. *Organic Chemistry*, 4th ed.; Brooks/Cole: Pacific Grove, CA, 1996; p 197. (b) Fox, M. A.; Whitesell, J. K. *Organic Chemistry*; Jones and Bartlett: New York, 1997; p 40. (c) Jones, M. J., Jr. *Organic Chemistry*; Norton and Co.: New York, 1997; p 134.

(12) Bernasconi, C. F.; Leyes, A. E. *J. Am. Chem. Soc.* **1997**, *119*, 5169.

(13) Bernasconi, C. F.; Leyes, A. E.; García-Río, L. *Organometallics* **1998**, *17*, 4940.

Discussion

General Features. The key steps in the synthesis of $3H^+(S)$ are shown in Scheme 1. The two methyl groups on the thiophene

Chart 1

Chart 2

(The charts contain chemical structures with the following labels and data.)

Chart 1 (left, reactions 10–17):

- **3H⁺(S)** ⇌ **3(S)**   ΔH° = 242.8 kcal/mol   (10)
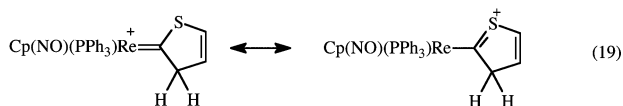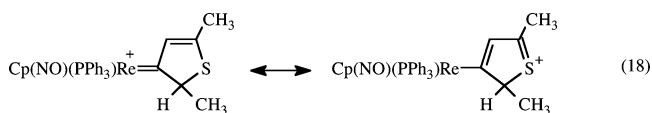- **4H⁺(S)′** ⇌ **4(S)′**   ΔH° = 244.6 kcal/mol   (11)
- **5H⁺(S)′** ⇌ **5(S)′**   ΔH° = 238.4 kcal/mol   (12)
- **6H⁺(S)′** ⇌ **6(S)′**   ΔH° = 239.5 kcal/mol   (13)
- **7H⁺(S)′** ⇌ **7(S)′**   ΔH° = 236.3 kcal/mol   (14)
- **8H⁺(S)′** ⇌ **8(S)′**   ΔH° = 237.4 kcal/mol   (15)
- **9H⁺(S)′** ⇌ **9(S)′**   ΔH° = 232.5 kcal/mol   (16)
- **1H⁺(S)′** ⇌ **1(S)′**   ΔH° = 233.9 kcal/mol   (17)

Chart 2 (right) structures with bond lengths: **3H⁺(S)′**, **3(S)′**, **4H⁺(S)′**, **4(S)′**, **5H⁺(S)′**, **5(S)′**, **6H⁺(S)′**, **6(S)′**, **7H⁺(S)′**, **7(S)′**, **8H⁺(S)′**, **8(S)′**, **9H⁺(S)′**, **9(S)′**, **1H⁺(S)′**, **1(S)′**.

3H⁺(S) and **1H⁺(S)**. One notable feature is the UV–vis spectrum of **3H⁺(S)**: the λ_{max} of 475 nm shows a large red shift compared to that of **1H⁺(S)** (412 nm[8]). This red shift is consistent with the push–pull conjugated system of **3H⁺(S)** (eq 18), which is more extended than that for **1H⁺(S)** (eq 19).

$$Cp(NO)(PPh_3)Re \quad \longleftrightarrow \quad Cp(NO)(PPh_3)Re \qquad (18)$$

$$Cp(NO)(PPh_3)Re \quad \longleftrightarrow \quad Cp(NO)(PPh_3)Re \qquad (19)$$

A similar red shift has been observed for **13** (λ_{max} 398 nm in DMF)[9] compared to **14** (λ_{max} 345 nm in MeCN);[10] again there

Chart 3

3H$^+$(S)′
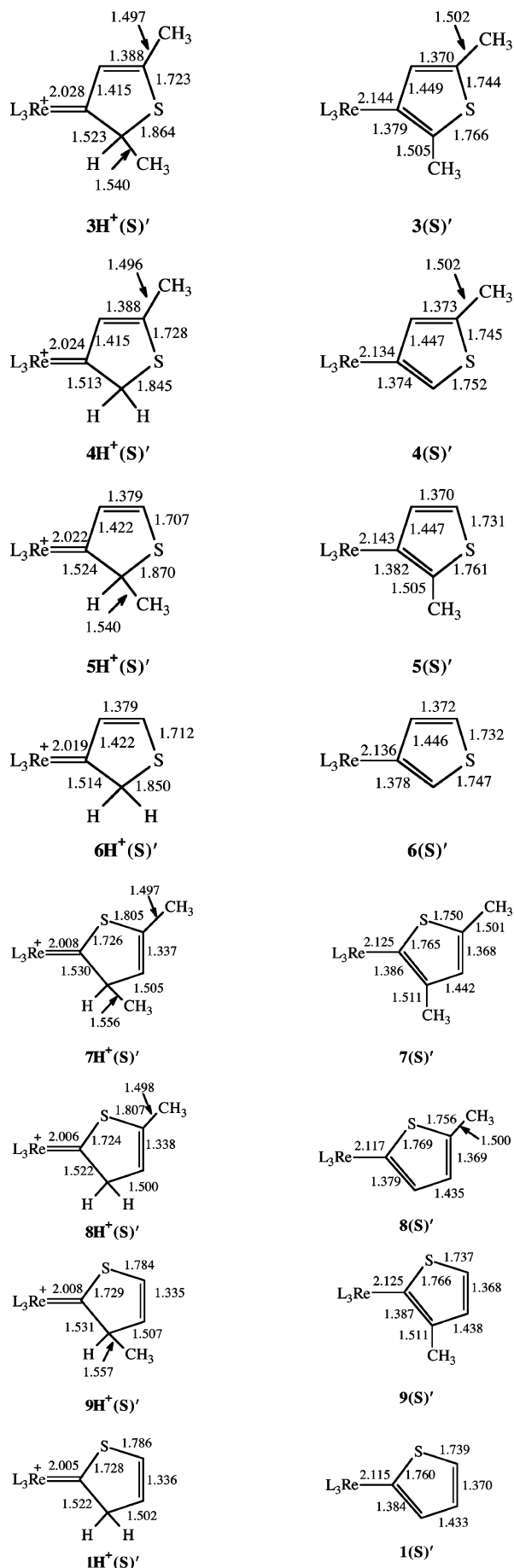
3(S)′

4H$^+$(S)′

4(S)′

5H$^+$(S)′

5(S)′

6H$^+$(S)′

6(S)′

7H$^+$(S)′

7(S)′

8H$^+$(S)′

8(S)′

9H$^+$(S)′

9(S)′

1H$^+$(S)

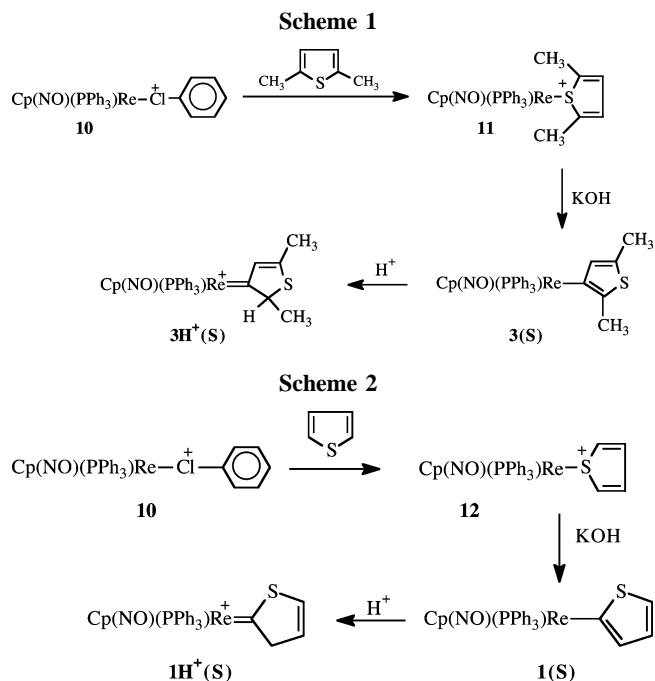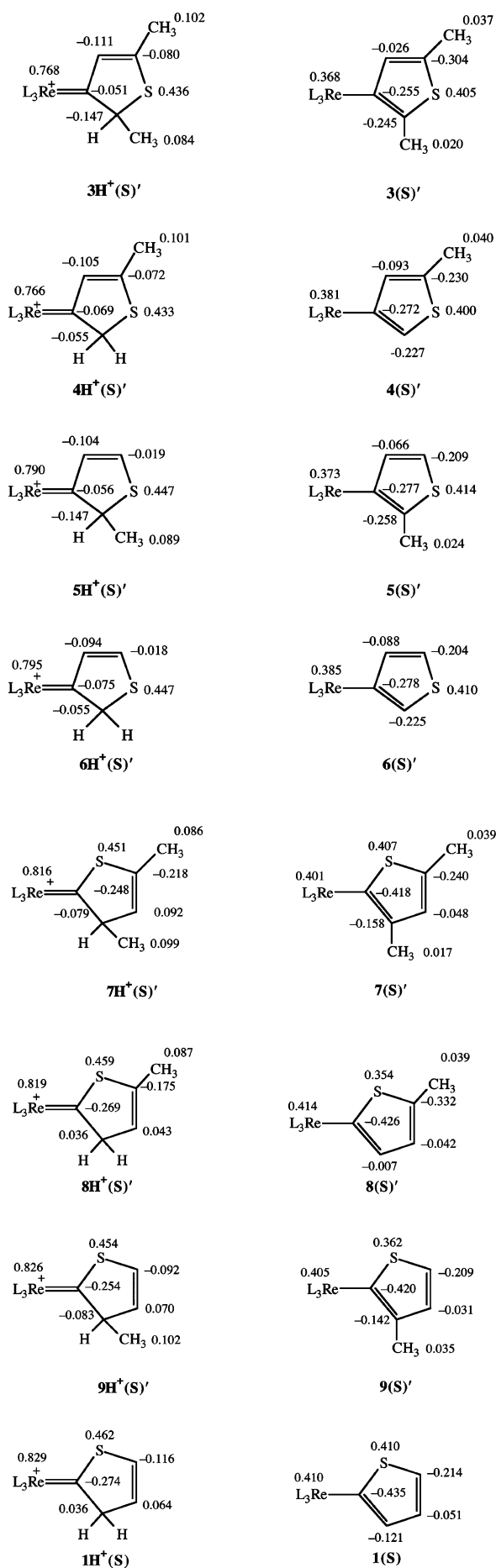1(S)

Scheme 1

10

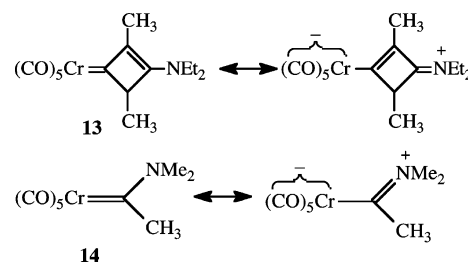11

3H$^+$(S)

3(S)

Scheme 2

10

12

1H$^+$(S)

1(S)

is a more extended π-system in **13** than in **14**.

13

14

X-ray versus Calculated Geometries. Table 1 summarizes the calculated geometric parameters for **3H$^+$(S)′** and **3(S)′** and those obtained by X-ray crystallography for **3(S)**. The calculated geometry for **3(S)′** is seen to be in good agreement with the experimental geometry of **3(S)**.

Values. The pK_a^{CH} value of **3H$^+$(S)** (2.64) is quite similar to that of **1H$^+$(S)** (2.51);[2] when the pK_a^{CH} of **1H$^+$(S)** is statistically corrected because **1H$^+$(S)** has two equivalent protons, one obtains pK_a^{CH}(corr) = 2.81. The fact that the acidities of the two carbene complexes are so similar is probably due to a fortuitous cancellation of competing factors. There are three main factors that could potentially affect the relative acidities of **3H$^+$(S)** and **1H$^+$(S)**. (1) The more extended π-system of **3H$^+$(S)** leads to a greater stabilization of this complex and should lower its acidity. (2) The methyl group on the α-carbon stabilizes the C=C double bond in **3(S)** that is formed upon deprotonation of **3H$^+$(S)**. This is a well-known features of alkenes[11] and should *increase* the acidity of **3H$^+$(S)**. If the comparison between **15** (pK_a^{CH}(corr) = 14.77)[12] and **16** (pK_a^{CH} = 13.41)[13] can serve as a guide, this acidifying effect of the methyl group may be quite significant. (3) The methyl group

15

16
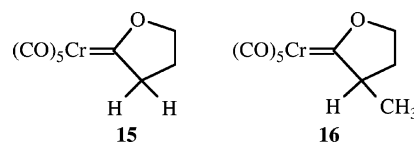
on the double bond adjacent to the sulfur atom may decrease the acidity of **3H$^+$(S)** by lowering the energy of the cation in

two ways. One is by stabilizing the C=C double bond, as is the case for **3(S)**, with the α-methyl group. The other is by stabilizing the positive charge on the resonance structure (B) and/or by hyperconjugation (C).
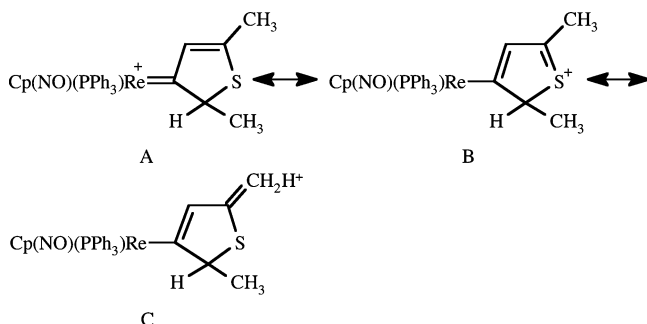

The calculated gas phase acidities of **1H⁺(S)′**, **3H⁺(S)′**, **4H⁺(S)′**, **5H⁺(S)′**, **6H⁺(S)′**, **7H⁺(S)′**, **8H⁺(S)′**, and **9H⁺(S)′** summarized in Chart 1 as well as the geometric parameters and group charges summarized in Charts 2 and 3, respectively, provide some insights into the potential importance of these factors.

From a comparison of systems with the skeleton of **6H⁺(S)′** to systems with the skeleton of **1H⁺(S)′** it is apparent that the more extended π-system indeed substantially lowers the acidity of the respective carbene complexes. The reductions in acidity amount to 6.5 kcal/mol (eq 10 vs 14), 7.2 kcal/mol (eq 11 vs 15), 5.9 kcal/mol (eq 12 vs 16), and 5.6 kcal/mol (eq 13 vs 17), respectively.

The predicted acidity enhancement by the α-methyl group can be seen by comparing eq 12 with eq 13 (1.4 kcal/mol) and eq 16 with eq 17 (1.4 kcal/mol); the postulated reduction in acidity by the other methyl group manifests itself by comparing eq 11 with eq 13 (5.1 kcal/mol) and eq 15 with eq 17 (3.5 kcal/mol). The combined effect of the two methyl groups is to decrease the acidity by 3.3 kcal/mol (eq 10 vs 13) and 2.4 kcal/mol (eq 14 vs 17), respectively.

The calculated geometries (Chart 2) and group charges (Chart 3) support the above interpretation of the structural effects on the stabilities of the various carbene complexes and their respective conjugate bases. (a) For the carbenes with the more extended π-systems (**3H⁺(S)′**, **4H⁺(S)′**, **5H⁺(S)′**, **6H⁺(S)′**) one would expect less double-bond character of the Re−C bond than for the other carbenes (**7H⁺(S)′**, **8H⁺(S)′**, **9H⁺(S)′**, **1H⁺(S)′**) due to the greater contribution of the resonance structures of the type **17** than those of the type **18**. This
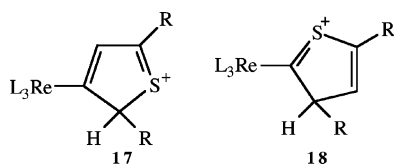
expectation is borne out by our calculations: for the former systems these bond lengths vary between 2.019 and 2.028 Å; for the latter they vary between 2.005 and 2.008 Å. At the same time there should also be greater charge delocalization in the first series, which should manifest itself in reduced charges on the groups at both ends of the conjugated system, i.e., the L₃Re moieties and the sulfur atoms. Indeed, for the carbenes with the more extended π-system the charges on the L₃Re moieties

(14) Reed, A. E.; Curtiss, L. A.; Weinhold, F. *Chem. Rev.* **1988**, *88*, 899.

Table 2. Rate Constants for the Reversible Deprotonation of 3H⁺(S) by Various Bases in 50% MeCN−50% Water (v/v) at 25 °C[a]

base	pK_a^{CH}	k_1^B, M⁻¹ s⁻¹	k_{-1}^{BH}, M⁻¹ s⁻¹
OH⁻	16.63	$(5.34 \pm 0.11) \times 10^1$	$(1.51 \pm 0.04) \times 10^{-11b}$
H₂O	−1.44	$(7.71 \pm 0.10) \times 10^{-3b}$	$(3.39 \pm 0.10) \times 10^0$
piperidine	11.01	$(1.16 \pm 0.01) \times 10^2$	$(4.94 \pm 0.09) \times 10^{-7}$
piperazine	9.97	$(2.54 \pm 0.01) \times 10^1$	$(1.19 \pm 0.01) \times 10^{-6}$
HEPA[c]	9.33	$(9.51 \pm 0.09) \times 10^0$	$(1.94 \pm 0.06) \times 10^{-6}$
morpholine	8.70	$(7.00 \pm 0.10) \times 10^0$	$(6.10 \pm 0.13) \times 10^{-6}$
PPAL[d]	8.15	$(3.63 \pm 0.05) \times 10^0$	$(1.12 \pm 0.02) \times 10^{-5}$
n-BuNH₂	10.40	$(5.88 \pm 0.08) \times 10^1$	$(1.02 \pm 0.02) \times 10^{-6}$
MeOCH₂CH₂NH₂	9.39	$(1.20 \pm 0.01) \times 10^1$	$(2.13 \pm 0.04) \times 10^{-6}$
H₂NCOCH₂NH₂	8.14	$(2.58 \pm 0.02) \times 10^0$	$(8.17 \pm 0.13) \times 10^{-6}$
ClCH₂CH₂NH₂	8.05	$(5.12 \pm 0.04) \times 10^0$	$(1.99 \pm 0.03) \times 10^{-5}$
NCCH₂NH₂	5.29	$(2.88 \pm 0.05) \times 10^{-1}$	$(6.34 \pm 0.16) \times 10^{-5}$
AcO⁻	5.93	$(2.93 \pm 0.06) \times 10^{-1}$	$(1.50 \pm 0.04) \times 10^{-4}$
MeOCH₂CO₂⁻	4.73	$(1.80 \pm 0.08) \times 10^{-1}$	$(1.46 \pm 0.08) \times 10^{-3}$
ClCH₂CO₂⁻	3.94	$(1.60 \pm 0.06) \times 10^{-1}$	$(8.04 \pm 0.37) \times 10^{-3}$

[a] $\mu = 0.1$ M (KCl). [b] In units of s⁻¹. [c] HEPA = 1-(2-hydroxyethyl)piperazine. [d] PPAL = 1-piperazinecarboxaldehyde.

are 0.768, 0.769, 0.792, and 0.795, while for the other carbenes they are 0.818, 0.819, 0.824, and 0.829, respectively; the charges on the sulfur atoms are 0.436, 0.433, 0.445, and 0.446 for the first series and 0.450, 0.458, 0.454, and 0.461, respectively, for the second series. (b) The somewhat larger positive charge on the methyl group attached to the C=C double bond compared to the methyl group on the α-carbon in **3H⁺(S)′** and in **4H⁺(S)′** versus **5H⁺(S)′** supports the notion that the methyl group on the C=C double bond helps stabilize **3H⁺(S)′** and **4H⁺(S)′** by absorbing part of the positive charge. However, the fact that the C−CH₃ bond lengths in **3H⁺(S)′** and **4H⁺(S)′** are not significantly different from the corresponding C−CH₃ bond lengths in **7H⁺(S)′** and **8H⁺(S)′** suggests that hyperconjugation (resonance structure C) is not a significant factor.

Gas Phase versus Solution Phase Acidities. The computational results are consistent with the notion that there are competing factors that affect the relative acidities of **3H⁺(S)** and **1H⁺(S)**. However, the factors that lead to a lowering of the acidity of **3H⁺(S)′** relative to **1H⁺(S)′** are dominant in the gas phase, while for **3H⁺(S)** versus **1H⁺(S)** in solution they are more balanced. A plausible explanation for this state of affairs is that there is less need for charge stabilization in **3H⁺(S)** by its more effective delocalization that results from the more extended π-system and by the methyl group attached to the C=C double bond because solvation helps stabilize the charge.

Rate Constants and Brønsted Parameters. The rate constants for the reversible deprotonation of **3H⁺(S)** are summarized in Table 2. The respective Brønsted plots are shown in

Figures 3−5, and the Brønsted coefficients are summarized in Table 3 along with those for the respective reactions of **1H⁺(S)**. The differences in the β and α values for the two carbene complexes are quite small and, for the reactions with the primary and secondary amines, lie well within the experimental uncertainties. Even for the reactions with the carboxylate ions the difference in the Brønsted coefficients is probably not mechanistically significant despite the fact that this difference is somewhat larger than the sum of the respective experimental uncertainties. On the other hand, the fact that β for the amine reactions is substantially larger than for the carboxylate reactions *is* significant and has been explained in terms of electrostatic effects at the transition state.[2]

Intrinsic Rate Constants. Marcus intrinsic rate constants (k_o)[15] were obtained from extrapolation of the Brønsted plots as $\log k_o = \log k_1^B/q = \log k_{-1}^{BH}/p$ at $pK_a^{BH} - pK_a^{CH} + \log$
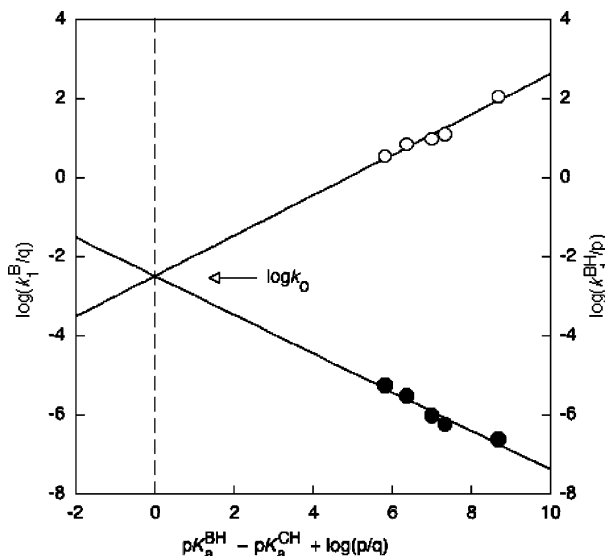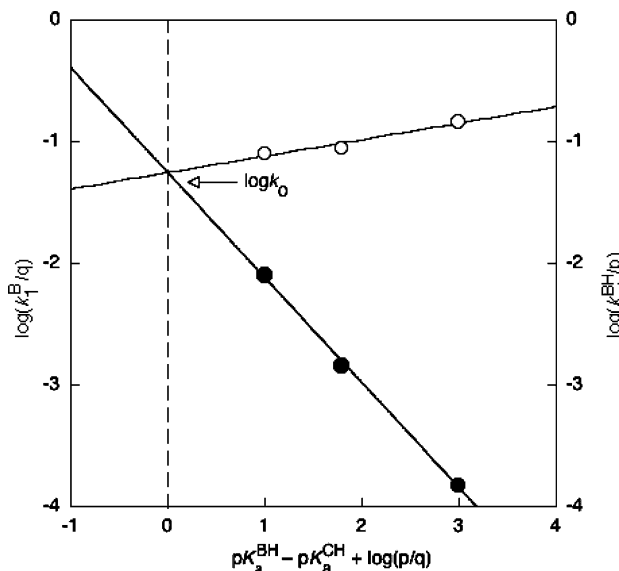
Figure 3. Brønsted plot for the reactions of $3H^+(S)$ with secondary alicyclic amines: (○) log k_1^B/q; (●) log k_{-1}^{BH}/p.
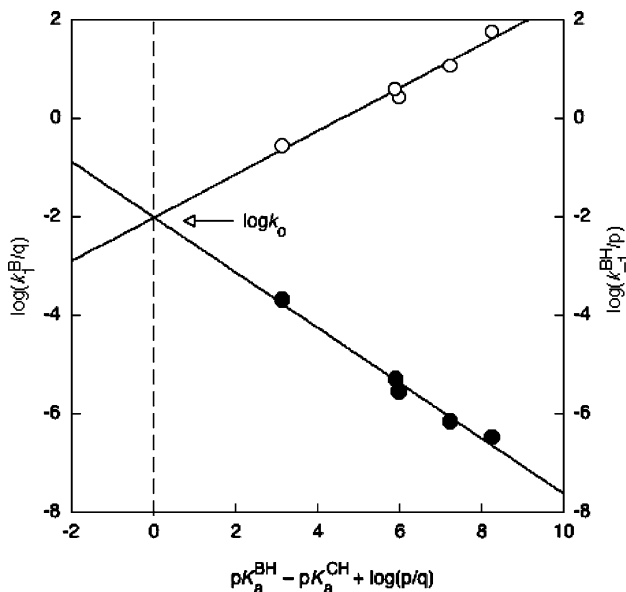
Figure 4. Brønsted plot for the reactions of $3H^+(S)$ with primary aliphatic amines: (○) log k_1^B/q; (●) log k_{-1}^{BH}/p.

$p/q = 0$. They are included in Table 3 along with those for the corresponding reactions of $1H^+(S)$. The differences between these log k_o values (Δlog k_o = log $k_o(3H^+(S))$ − log $k_o(1H^+(S))$) are −2.46 ± 0.10 for the carboxylate ions, −2.25 ± 0.64 for the primary amines, and −3.54 ± 1.01 for the secondary amines. Because of the large experimental uncertainties in some of these Δlog k_o values, no firm conclusion can be reached regarding the dependence of Δlog k_o on the type of buffer, even though the large Δlog k_o for the secondary alicyclic amines suggests a larger reactivity difference for these amines than for the other buffers, which can be attributed to a steric effect (more on this below). Hence we shall mainly focus our discussion on the fact that for all buffer types log k_o for $3H^+(S)$ is substantially lower than for $1H^+(S)$. The same is

(15) The Marcus[16] intrinsic rate constant, k_o (Marcus intrinsic barrier, $\Delta G_o^\ddagger$), of a reaction with a forward rate constant k_1 and a reverse rate constant k_{-1} is defined as $k_o = k_1 = k_{-1}$ when $K_1 = 1$ ($\Delta G_o^\ddagger = \Delta G_{-1}^\ddagger$ when $\Delta G° = 0$). For proton transfers, statistical factors p (number of equivalent protons on BH^+) and q (number of equivalent basic sites on B) are usually included.[17]

Figure 5. Brønsted plot for the reactions of $3H^+(S)$ with carboxylate ions: (○) log k_1^B/q; (●) log k_{-1}^{BH}/p.

Table 3. Brønsted Coefficients and Intrinsic Rate Constants

carbene complex	pK_a^{CH}	base type	β	α	logk_o[a]
Cp(NO)(PPh₃)Re⁼ (structure) $(3H^+(S))$	2.64	RCOO⁻	0.14 ± 0.03	0.86 ± 0.03	−1.25 ± 0.7
		RNH₂	0.44 ± 0.05	0.56 ± 0.05	−1.98 ± 0.30
		R₂NH	0.51 ± 0.07	0.49 ± 0.07	−2.49 ± 0.47
Cp(NO)(PPh₃)Re⁼ (structure) $(1H^+(S))$[b]	2.51	RCOO⁻	0.21 ± 0.02	0.79 ± 0.02	1.21 ± 0.03
		RNH₂	0.42 ± 0.05	0.58 ± 0.05	0.27 ± 0.34
		R₂NH	0.40 ± 0.07	0.60 ± 0.07	1.05 ± 0.54

[a] Δlog k_o = log $k_o(3H^+(S))$ − log $k_o(1H^+(S))$ = −2.46 ± 0.010 (RCOO⁻), −2.25 ± 0.64 (RNH₂), −3.54 ± 1.01 (R₂NH). [b] Reference 2.

Table 4. Rate Constants for the Reactions with OH⁻ and Water as the Base; Approximate Δlog k_o Values

base	$k_1^B(3H^+(S))$	$k_1^B(1H^+(S))$	$\dfrac{k_1^B(3H^+(S))}{k_1^B(1H^+(S))}$	Δlog k_o[a]
OH⁻	5.34×10^1 M⁻¹ s⁻¹	2.37×10^4 M⁻¹ s⁻¹	2.25×10^{-3}	≈−2.6
H₂O	7.71×10^{-3} s⁻¹	2.02×10^{-1} s⁻¹	3.82×10^{-2}	≈−1.4

[a] Δlog k_o = log $k_o(3H^+(S))$ − log $k_o(1H^+(S))$ ≈ log$(k_1^B(3H^+(S))/k_1^B(1H^+(S)))$.

true for the reactions with water or OH⁻ as the base (Table 4). There are several factors that are likely to contribute to this difference.

(1) The stabilization of the C⁼C double bond in $3(S)$ by the α-methyl group (see discussion of the pK_a^{CH} values) is not matched by a proportional stabilization of the transition state because the development of the C⁼C double bond between the α-carbon and the carbene carbon lags behind proton transfer (19).[18] According to the principle of nonperfect synchronization
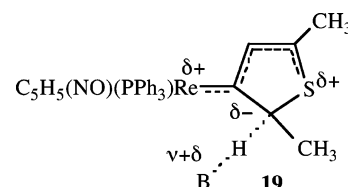
(PNS),[19] this leads to a lowering of the intrinsic rate constant.[21]

(16) Marcus, R. A. *J. Phys. Chem.* **1968**, *72*, 891.

In addition, there is a *de*stabilization of the transition state, not present in either reactant or product, because of the unfavorable interaction between the inductively electron-donating methyl group and the partial negative charge in the α-carbon. This feature lowers k_o further. Similar effects on the intrinsic rate constants of proton transfers have been observed when comparing **16**[13] with **15**,[12] and **21**[22] with **20**;[22] these observations are

20   **21**
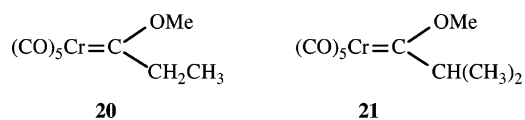
also reminiscent of what has been called the "nitroalkane anomaly", where the comparison is between nitromethane, nitroethane, and 2-nitropropane.[23]

(2) More severe steric crowding in the transition state for the reactions of **3H⁺(S)** is likely to contribute to the reduction in k_o for this carbene complex. Another manifestation of this steric effect is that $k_o(R_2NH) < k_o(RNH_2)$ for the reactions of **3H⁺(S)**, but $k_o(R_2NH) > k_o(RNH_2)$ for the reactions of **1H⁺(S)**. The latter situation is "normal" for uncrowded systems[24] and reflects a solvation effect;[25] for highly crowded systems the solvation effect is more than offset by the steric effect. A similar situation exists in the reaction of **21** with piperidine[22] as well as in other systems,[27] and this is why the larger $\Delta\log k_o$ value for the secondary alicyclic amines mentioned above is probably a genuine finding despite the large experimental uncertainty.

(3) The closer proximity of the sulfur atom to the α-carbon in **3H⁺(S)** than in **1H⁺(S)** may possibly provide a kinetic advantage to **3H⁺(S)**. This is because the electron-withdrawing inductive effect of the sulfur may serve to stabilize the partial negative charge on the α-carbon at the transition state; since this effect is essentially nonexistent in the product, there should be an increase in the intrinsic rate constant for **3H⁺(S)**. Our

results show that this effect cannot be very important and is more than offset by factors 1 and 2.

Conclusions

(1) **3H⁺(S)**, a novel Fischer carbene complex, has been synthesized and fully characterized. Although it hydrolyzes rapidly in the presence of water, it can be reversibly deprotonated in pure acetonitrile and, by using a stopped-flow apparatus, even in 50% MeCN−50% water (v/v). Its conjugate base, **3(S)**, a known compound, is more stable and its X-ray structure is reported.

(2) The pK_a^{CH} of **3H⁺(S)** (2.64) is nearly identical to the pK_a^{CH} of **1H⁺(S)** (2.51). This is most likely the result of a fortuitous cancellation of the acidity-enhancing stabilization of **3(S)** by the α-methyl group and the acidity-reducing stabilization of **3H⁺(S)** resulting from the more extended π-system compared to that of **1H⁺(S)** and the methyl group attached to the C=C double bond. This notion is supported by DFT calculations on **3H⁺(S)′**, **1H⁺(S)′**, and several model compounds.

(3) The intrinsic rate constants for the deprotonation of **3H⁺(S)** by amines and carboxylate ions are about 2 orders of magnitude lower than for the deprotonation of **1H⁺(S)** by the same bases. The same is true for deprotonation by OH⁻ and by water. This reduction is attributed to a combination of several factors: (a) a PNS effect resulting from the lag in the development of the C=C double bond, which prevents the transition state from benefiting from the stabilization of this double bond by the α-methyl group; (b) a destabilization of the transition state group due to the unfavorable interaction of the α-methyl group with the partial negative charge on the α-carbon; (c) a steric effect because there is more crowding at the transition state for the deprotonation of **3H⁺(S)** than for the deprotonation of **1H⁺(S)**. This effect is particularly strong with the bulky secondary alicyclic amines.

Experimental Section

Synthesis of 3H⁺(S). The BF₄⁻ salt of **3H⁺(S)** was prepared by protonation of **3(S)** as follows. To a degassed, stirred, and cooled (-42 °C) solution of 0.15 mmol of **3(S)** in 12 mL of ether−CH₂Cl₂ (2:1) was added 1 equiv of HBF₄·OMe₂. The orange-red solution immediately turned deep orange, and within 30 min an orange precipitate began to form. After stirring for 2 h, 60 mL of ether−hexane (1:1) was added. The resulting precipitate was filtered and washed with 2 × 10 mL of ether−hexane (1:1). The precipitate was dried under N₂ while being allowed to warm to room temperature and then dried in vacuo; yield 90%. Note that **3H⁺(S)** is moisture and air sensitive and was stored under argon. ¹H NMR δ (CD₂Cl₂): 1.57 (d, α-CH₃), 2.33 (s, vinylic CH₃), 4.17 (q, α-H), 5.33 (s, vinylic H), 5.80 (s, Cp), 7.11, 7.22−7.33, 7.50−7.65 (m, Ph). ¹³C NMR δ (CD₂Cl₂): 18.62 (CH₃−C(2)), 24.60 (CH₃−(C5)), 72.36 (C(2)), 97.21 (Cp), 130.09 (Ph), 131.05 (Ph), 132.56 (Ph), 133.20 (Ph), 146.59 (C(4)), 179.29 (C(5)), 282.02 (C(3), carbene carbon). IR cm⁻¹ ν(NO) (CH₂Cl₂): 1700.8 (s). MS: 656.16 (M⁺), 585.17 (M⁺ − NO), 544.16 M⁺ − 2,5-dimethylthiophene). UV (CH₂Cl₂): 478 nm (log ϵ 4.01).

Synthesis of 3(S). The synthesis of **3(S)** followed the procedure (method A) described by Robertson, White, and Angelici.[3a]

X-ray Structure of 3(S). A red-orange prism of dimensions 0.18 × 0.22 × 0.29 mm³ was mounted in the 91(2) K nitrogen cold stream provided by CRYO Industries low-temperature apparatus on the goniometer head of a Bruker SMART 1000 diffractometer. Diffraction data were collected with graphite-monochromated Mo Kα radiation employing 0.3° ω scans and approximately a full sphere of data to $2\theta_{max}$ of 61°. A multiscan correction for absorption

(17) Keeffe, J. R.; Kresge, A. J. In *Investigation of Rates and Mechanisms of Reactions*; Bernasconi, C. F., Ed.; Wiley-Interscience: New York; Part I, p 747.

(18) As is generally the case in proton transfers from carbon acids activated by π-acceptor groups, the transition state is undoubtedly imbalanced in the sense that π-bond formation to the π-acceptor and delocalization of the negative charge into the π-acceptor group lags behind proton transfer.[19] This has been shown to be true for Fischer carbene complexes as well.[20] In the present case, this lag implies that π-bond formation between the α-carbon and the carbene carbon has made little progress at the transition state (**19**).

(19) (a) Bernasconi, C. F. *Acc. Chem. Res.* **1987**, *20*, 301. (b) Bernasconi, C. F. *Acc. Chem. Res.* **1992**, *25*, 9. (c) Bernasconi, C. F. *Adv. Phys. Org. Chem.* **1992**, *27*, 119.

(20) (a) Bernasconi, C. F.; Sun, W. *J. Am. Chem. Soc.* **2002**, *124*, 2299. (b) Bernasconi, C. F. *Adv. Phys. Org. Chem.* **2002**, *37*, 137.

(21) In the context of a proton transfer reaction, the PNS states that the intrinsic rate constant decreases if the development of a product-stabilizing factor lags behind the proton transfer but increases if the development of the product-stabilizing factor runs ahead of the proton transfer.[19]

(22) Bernasconi, C. F.; Sun, W.; García-Río, L.; Kin-Yan; Kittredge, K. *J. Am. Chem. Soc.* **1997**, *119*, 5583.

(23) Kresge, A. J. *Can. J. Chem.* **1974**, *52*, 1897.

(24) The higher k_o values for secondary amines is caused by differences in the solvation energies of the respective protonated amines and the fact that at the transition state solvation of the incipient ammonium ion lags behind proton transfer.[25,26] Note that this effect is a manifestation of the PNS.[19]

(25) Bell, R. P. *The Proton in Chemistry*, 2nd ed.; Cornell University Press: Ithaca, NY, 1973; Chapter 10.

(26) Jencks, W. P. *Catalysis in Chemistry and Enzymology*; McGraw-Hill: New York, 1968; p 178.

(27) (a) Farrell, P. G.; Terrier, F.; Xie, H.-Q.; Boubaker, T. *J. Org. Chem.* **1990**, *55*, 2546. (b) Terrier, F.; Xie, H.-Q.; Lelièvre, J.; Boubaker, T.; Farrell, P. G. *J. Chem. Soc., Perkin Trans. 2* **1990**, 1899.

was applied using the program SADABS 2.10.[28] A total of 23 467 reflections were collected, of which 7680 were unique [R(int) = 0.023] and 6905 were observed [($I > 2\sigma(I)$]. The structure was solved by direct methods (SHELXS-97[28]) and refined by full-matrix least-squares of F_2 (SHELXL97[28]) using 309 parameters. All non-hydrogen atoms were refined with anisotropic thermal parameters. The H atoms on C atoms were generated geometrically and refined as riding atoms with C–H = 0.95–1.00 Å and U_{iso}(H) = 1.2 times U_{eq}(C) for CH and CH₂ groups and U_{iso}(H) = 1.5 times U_{eq}(C) for CH₃ groups. The maximum and minimum peaks in the final difference Fourier map were 1.87 e Å^{-3} (near Re) and -0.72 e Å^{-3}. Crystal data: $C_{29}H_{27}NOPReS$, MW = 654.75, monoclinic $C2/c$, $a = 31.471(4)$ Å, $b = 10.3616(12)$ Å, $c = 18.8840(19)$ Å, $\beta = 124.664(7)°$, $V = 5064.9(10)$ Å^3, $T = 91(2)$ K, $Z = 8$, R_1 [$I > 2\sigma(I)$] = 0.0185, wR_2 (all data) = 0.0472, GOF (on F^2) = 0.992.

Materials. The solvents and buffers used in this study were obtained from the same sources and purified in the same manner as before.[1]

Procedures. pH measurements,[29] recording of spectra, and kinetic experiments were performed essentially as described in previous papers;[1,2,31] see also footnotes in Tables S6–S20[4] for more details. Due to the rapid decomposition of **3H**⁺(**S**) in aqueous acetonitrile, the stopped-flow kinetic experiments could not be run using the standard procedure of initiating the reaction by mixing substrate and buffer each in 50% MeCN–50% water. Instead, one syringe contained the substrate in pure acetonitrile while the other contained the buffer in water. It was shown that the optical artifacts that can occur when mixing two different solvents were minimal and did not affect the kinetic traces.

Calculations. All computations were carried out using the GAUSSIAN suite of programs.[32] ChemDraw and Chem3D were used to construct starting geometries for the rhenium complexes. Cartesian coordinates were transferred to Gaussian input format and optimized. Generalized basis sets were employed for the final optimizations. 6-31+G(d) was applied to the carbon and sulfur atoms in the thiophene structures. 6-31 was applied to the rest of the atoms. Rhenium was treated with an effective core potential Hay–Wadt (n+1) ECP VDZ basis set[33] obtained from the Extensible Computational Chemistry Environment Basis Set Database.[34] This allowed for explicit treatment of the valence electrons on rhenium, while lower-lying electrons are treated as implicit electric fields. Local minima were found in which the rhenium–nitrogen–oxygen angle was found to be approximately 90.0°. These structures were artifacts of early optimizations using nonpolarizable basis sets. In the penultimate steps for optimization the rhenium–nitrogen–oxygen angles were constrained to approximately 180.0°. Finally all coordinates were allowed to optimize at the B3LYP level, yielding the structures given in the Supporting Information.

Supporting Information Available: Tables S1–S5 (crystal structure parameters), S6–S20 (kinetic data), and S21–S45 (DFT calculations); complete ref 32. This material is available free of charge via the Internet at http://pubs.acs.org.

OM0604369

(28) Sheldrick, G. M. *SHELXL97, SHELXS-97, SADABS 2.10*; University of Göttingen: Göttingen, Germany, 1997.

(29) The pH was determined as pH(measured) + 0.18 according to Allen and Tidwell.[30]

(30) Allen, D. A.; Tidwell, T. T. *J. Am. Chem. Soc.* **1987**, *109*, 2774.

(31) Bernasconi, C. F.; Ali, M. *J. Am. Chem. Soc.* **1999**, *121*, 3039.

(32) Frisch, M. J. et al. *GAUSSIAN 03*, Revision B.04.

(33) Hay, P. J.; Wadt, W. R. *J. Chem. Phys.* **1985**, *82*, 299.

(34) Extensible Computational Chemistry Environment Basis Set Database, Version 02/25/04, as developed and distributed by the Molecular Science Computing Facility, Environmental and Molecular Sciences Laboratory, which is part of the Pacific Northwest Laboratory, P.O. Box 999, Richland, WA 99352, and funded by the U.S. Department of Energy. The Pacific Northwest Laboratory is a multiprogram laboratory operated by Battelle Memorial Institute for the U.S. Department of Energy under contract DE-AC06-76RLO 1830.